

Charge Distribution and UV Absorption Spectra of Liquid Crystals with Structural Element $[closo-B_{10}H_{10}]^{2-}$: A Theoretical Approach

P. Lakshmi Praveen¹, Ramakrishna D. S.²

Department of Physics, Veer Surendra Sai University of Technology, Burla, Sambalpur, Odisha, India.¹

Department of Chemistry, Veer Surendra Sai University of Technology, Burla, Sambalpur, Odisha, India.²

Abstract: The present work reports the UV absorption spectral characteristics, and charge distribution analysis of two liquid crystal molecules *viz.*, 1-Dinitrogen-10-(4-pentyl-1-quinuclidinyl)-*closo*-decaborate (NCDB), and 1-Dinitrogen-10-(4-pentyl-1-thiacyclohexyl)-*closo*-decaborate (SCDB). Mulliken and Loewdin population analysis have been performed to understand the charge distribution of the molecules. The electronic transitions, ultraviolet (UV) absorption wavelengths, HOMO (highest occupied molecular orbital) and LUMO (lowest unoccupied molecular orbital) energies have been reported. Further, charge distribution, and UV stability of the molecules has been discussed in the light of partial atomic charges, absorption wavelength and electronic transition oscillator strength (f) respectively.

Keywords: Charge distribution, HOMO, LUMO, Oscillator strength.

I. INTRODUCTION

Liquid crystals (LCs) are anisotropic fluids formed by anisometric molecules typically containing both a rigid core and flexible substituents, *e.g.* alkyl chains. Typically, the molecular core contains cyclic elements, such as benzene ring, cyclohexane, bicyclo-[2.2.2] octane, or a heterocycle substituted in the antipodal positions. The rigid core elements may be connected directly or linked through functional groups such as esters, imines, and azo or ethylene spacers. In such systems, liquid crystallinity appears as a balance between ordering forces of the rigid cores, and disordering effects of the alkyl chains [1]. Rod-like molecules typically form nematic and smectic phases. The nematic phase is the least organized phase, but it is the most widely employed in the display industry [2].

Boron cluster species are very expensive, and find practical applications only in some exclusive areas where no alternative exists. The compounds of boron exhibit some correspondence with the compounds of carbon, but also preserve some differences. Due to the combination of similarities with differences, boron plays as an excellent structural element in design and synthesis of new compounds [3]. The discovery of polyhedral boron clusters updates the way of perceptive the chemical bonding. The unique bonding characteristics of boron clusters cause σ -aromaticity, and the exceptional phase stability. The availability of the boron cluster species like pentaborane, decaborane, and icosahedral boranes have limited availability, and their revival in industrial production has been occurred after the development of some important applications. These properties and applications opened up the possibilities of boron clusters in the fields of display industry, nuclear research, and reactor technology [4]. The *closo*-borates have dominated the field due to their availability and relative ease of functionalisation. An additional advantage of boron clusters and their metal complexes is that they are abiotic,

therefore, chemically and biologically orthogonal to native cellular components, and usually resistant to catabolism, which is desirable property of biological applications [5]. In spite of the enormous potential of boron compounds, the modification of physiologically active species has not been generally recognized. The transparency to UV light of these systems along with the chemical and optical stability has not been well understood.

In view of this, the present article has been aimed to understand the phase stability, and UV stability of the NCDB, SCDB molecules in the light of charge distribution, absorption wavelength and electronic transition oscillator strength (f) respectively. Further, it concentrates on the correlation in molecular structures. The HOMO, LUMO energies, oscillator strength (f) have also been reported. An examination of thermodynamic data has revealed that NCDB, SCDB molecules exhibits nematic phase [6].

II. MOLECULAR MODELS AND METHOD

The present study adopts DFT method for the estimation of spectral shifts of NCDB and SCDB molecules. An efficient and widely used technique to study a molecular structure is DFT. This method with B3LYP/6-31 + G(d) level of calculation has been applied to optimise the molecules in the gas phase. The B3LYP (Becke–Lee–Yang–Parr) version of DFT is the combination of Becke's three parameter non-local hybrid functional of exchange terms [7] with the Lee, Yang and Parr correlation functional. The basis set of 6-31+G (d) contains a reasonable number of basis set functions. The geometry optimizations have been performed using the density functional theory (DFT) approach without symmetry constraints. The DFT approach was originally developed by Hohenberg and Kohn [8], Kohn and Sham [9, 10] to provide an efficient method of handling many-electron

system. For singlet ground states, DFT calculations have been performed using the B3LYP functional. According to DFT, the electron density is the fundamental properties of molecular and electronic system; however electron density alone could not define the entire chemical phenomenon. It's sensitivity to structural perturbation, and response to the changes in external condition are rather more important in reflecting the chemical reactivity of a system rather than the absolute value of electron density.

For singlet excited states, the excitation energies and oscillator strengths at the optimised geometry in the ground state have been obtained by TDDFT calculations with the B3LYP functional coupled with the configuration interaction (CI) single level of approximation including all $\pi \rightarrow \pi^*$ single excitations. This has been found adequate to determine the UV-Visible absorption spectra [11, 12] provided that suitable parameterizations are used. The DFT calculations have been performed by a spectroscopy oriented configuration interaction procedure (SORCI) [13]. Further, HOMO (H), LUMO (L) energies, energy gap ($E_g = E_L - E_H$) have been reported. The general structural parameters of the systems such as bond lengths, and bond angles have been taken from published crystallographic data [6].

III. RESULTS AND DISCUSSION

The molecular structures of NCDB, SCDB molecules have been shown in Fig. 1.

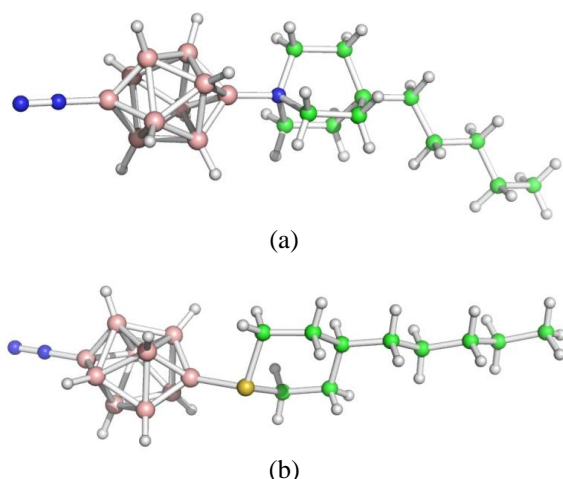


Fig. 1. Molecular structures of NCDB, SCDB molecules.

In order to obtain more information on the reactivity of above molecules towards nucleophile and electrophile, we performed DFT based calculation to evaluate the negative and positive charge distributions. Mulliken and Loewdin population analysis have been performed to understand the charge distribution in these molecules. Electrical charges in the molecule are obviously the driving force of electrostatic interactions. Indeed, it has been proven that local electron densities or charges are important in many chemical reactions, and physicochemical properties of compounds. Atomic partial charges have been used as static chemical reactivity indices [14]. The analysis has been given below:

3.1. Charge Distribution

(a) NCDB:

The charge distribution of NCDB molecule based on Mulliken, and Loewdin population analysis have been shown in Fig. 2. Mulliken data shows that there are thirty five positive charge atoms including one carbon, one nitrogen, nine boron atoms, and the other twenty four hydrogen atoms. Thus, there are eleven positive charge sites for nucleophilic attack. The decreasing order of reactivity of these sites for nucleophilic attack is B37 (0.172) > B54 (0.072) > N55 (0.051) > B44 (0.022) > B38 (0.021) > B42 (0.019) > B40 (0.017) > B50 (0.010) > B52 (0.008) > C2 (0.006) > B48 (0.004). The most positive position in NCDB is B37 ($Q_{MAX}=0.172$), and the lowest positive position is B48 ($Q_{MIN}=0.004$). It has been shown in the Fig. 2 that there are twenty one negative charge sites for electrophilic attack. The decreasing order of reactivity of these sites for electrophilic attack, the most, and the lowest negative charge sites may be understood from the Fig. 2. Similarly, the Loewdin analysis data may also be analyzed for the same data.

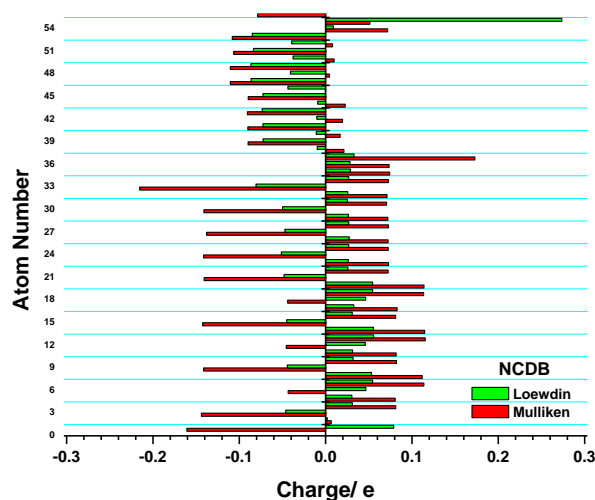


Fig. 2. Charge distribution of NCDB molecule.

(b) SCDB:

The charge distribution of SCDB molecule based on Mulliken, and Loewdin population analysis have been shown in Fig. 3. Mulliken data shows that there are thirty one positive charge atoms including one nitrogen, ten boron atoms, and the other twenty hydrogen atoms. Thus, there are eleven positive charge sites for nucleophilic attack. The decreasing order of reactivity of these sites for nucleophilic attack is B13 (0.163) > B4 (0.089) > N2 (0.054) > B5 (0.023) > B10 (0.022) > B7 (0.019) > B12 (0.018) > B8 (0.016) > B9 (0.013) > B6 (0.012) > B11 (0.009). The most positive position in SCDB is B13 ($Q_{MAX}=0.163$), and the lowest positive position is B11 ($Q_{MIN}=0.009$). It has been shown in the Fig. 3 that there are twenty negative charge sites for electrophilic attack. The decreasing order of reactivity of these sites for electrophilic attack, the most, and the lowest negative charge sites may be understood from the Fig. 3. Similarly, the Loewdin analysis data may also be analyzed for the same data.

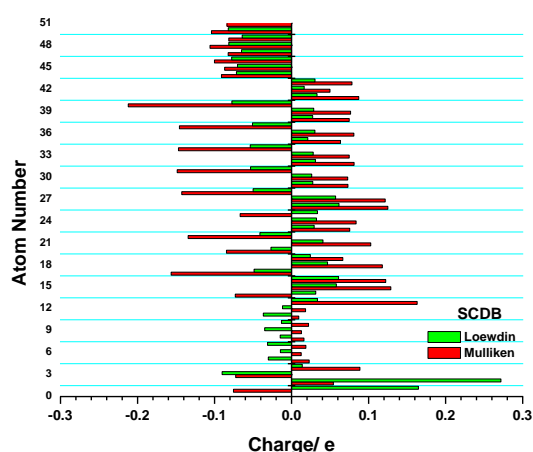


Fig. 3. Charge distribution of SCDB molecule.

3.2. UV Absorption Spectra:

(a) NCDB:

The UV absorption spectrum of NCDB molecule has been shown in Fig. 4 using DFT method.

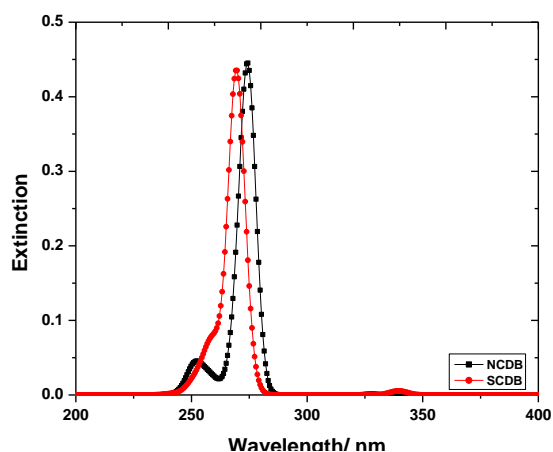


Fig. 4. UV absorption spectra of NCDB, SCDB molecules.

A two-band structure has been observed in the UV region with absorptions at 252.15nm (λ_1), and 274.41nm (λ_2). However, no absorption has been observed in the visible region. The strongest band appears in a region of 263.23nm to 286.13 with absorption maxima (λ_{max}) at 274.41nm.

This band arises from the HOMO→LUMO transition, and is assigned as $\pi \rightarrow \pi^*$ transition in the molecule. The other absorption band corresponding to the remaining wavelengths in UV region also indicate the possibility of $\pi \rightarrow \pi^*$ transitions in the molecule at higher wavelengths. The oscillator strengths (f) of these two absorptions corresponding to λ_1, λ_2 , are 0.02, and 0.43 respectively. Therefore, these transitions contribute the highest oscillator strength corresponding to absorption band at λ_2 . The extinction coefficients and vertical transition energies have been reported in Table 1.

(b) SCDB:

The UV absorption spectrum of SCDB molecule has been shown in Fig. 4 using DFT method. A two-band structure has been observed in the UV region with absorptions at 269.73nm (λ_1), and 340.04nm (λ_2). However, no absorption has been observed in the visible region. The strongest band appears in a region of 244.53nm to 282.62nm with absorption maxima (λ_{max}) at 269.73nm. This band arises from the HOMO→LUMO transition, and is assigned as $\pi \rightarrow \pi^*$ transition in the molecule. The other absorption band corresponding to the remaining wavelengths in UV region also indicate the possibility of $\pi \rightarrow \pi^*$ transitions in the molecule at higher wavelengths. The oscillator strengths (f) of these two absorptions corresponding to λ_1, λ_2 , are 0.43, and 0.005 respectively. Therefore, these transitions contribute the highest oscillator strength corresponding to absorption band at λ_1 . The extinction coefficients and vertical transition energies have been reported in Table 1.

The strongest absorption band for both molecules has been found in almost same region, which indicates the similar π -electron structure. Further, the HOMO, LUMO, and energy gap values have been reported in Table 1. The oscillator strength is a dimensionless quantity that expresses the probability of absorption of electromagnetic radiation in transitions between energy levels of an atom or molecule.

Table 1. The absorption bands (AB), extinction coefficients (EC), Oscillator strength (f), Vertical transition energy (EV), HOMO (H), LUMO (L) energies, and the band gap ($E_g = EL - EH$) of NCDB, and SCDB molecules using DFT method.

Molecule	Absorption Bands/ nm	EC*	f	E_V / eV
NCDB	252.15	0.04	0.02	4.92
	274.41	0.44	0.43	4.52
	H = -7.66eV; L = -1.02eV; $E_g = 6.64$ eV			
SCDB	269.73	0.43	0.39	4.60
	340.04	0.005	0.002	3.63
	H = -7.83eV; L = -1.12eV; $E_g = 6.71$ eV			

Bold value represents λ_{max}/nm

*EC unit: $10^4 \text{ dm}^3 \text{ mol}^{-1} \text{ cm}^{-1}$

It indicates the allowedness of electronic transitions in a molecule, and it is particularly valuable as a method of comparing 'transition strengths' between different types of quantum mechanical systems. It may be observed from the Table 1 that NCDB molecule exhibits the higher oscillator strength at 274.41nm, and SCDB molecule at 269.73nm.

This indicates the much flexibility of NCDB molecule for electronic transitions over a long wavelength region, and high photo sensitivity for this molecule, which may be exploited for optical, electronic applications. The continuous decrease in absorption and oscillator strength clearly after λ_2 , and λ_1 for NCDB, and SCDB indicates the breakage of the molecules with respect to the higher wavelengths, and subsequently losing the photo sensitivity. These important aspects of the spectra of these molecules are expected from the correlations in molecular structures. This may be explored for desired applications.

IV. CONCLUSION

The charge distribution, and UV absorption spectra of two liquid crystals with structural element $[c\text{loso-B}_{10}\text{H}_{10}]^{2-}$ leads to the following conclusions:

1. Both the molecules contain equal number of positive charge sites for nucleophilic attack. The NCDB molecule has highest and lowest positive atomic sites.
2. NCDB molecules exhibits higher absorption wavelength, and oscillator strength, hence, exhibits the high photo sensitivity.
3. The energy gap determines the molecular reactivity such as the ability to absorb light, and to react with other species, a molecule with small gap (NCDB in this case) is expected to have higher reactivity, and a lower stability in photo-physical processes.

REFERENCES

1. Lakshmi Praveen, P., Ojha, D. P. The Influence of alkyl chain length and solvents on configurational probability of liquid materials – A computational approach, *Mol. Cryst. Liq. Cryst.* 2015, 608, 72-81.
2. Hariprasad, S., Srinivasa, H. T. Symmetric 3, 5-pyrazole and isoxazole heterocycles comprising a bent core unit: Synthesis and mesomorphic characterization, *Liq. Cryst.* 2015, 42, 1612-1620.
3. Jose, T. J., Simi, A., Raju, M. D., Praveen, P. L. Liquid crystalline carborane diester molecules: Structure and ultraviolet absorption behaviour based on DFT and semiempirical methods, *Int. Adv. Res. J. Sci. Engg. Technol.* 2015, 2, 14-20.
4. Hosmane, N. S. (Ed.), *Boron Science: New Technologies and Applications*, CRC Press, London, 2012.
5. Liu, X., Yang, Q., Bao, Z., Su, B., Zhang, Z., Ren, Q., Yang, Y., Xing, H. Nonaqueous lyotropic ionic liquid crystals: Preparation, characterization, and application in extraction, *Chem. Eur. J.* 2015, 21, 9150-9156.
6. Jankowiak, A., Baliński, A., Harvey, J. E., Mason, K., Januszko, A., Kaszyński, P., Young, Jr. V. G., Persoons, A. $[c\text{loso-B}_{10}\text{H}_{10}]^{2-}$ as a structural element for quadrupolar liquid crystals: a new class of liquid crystalline NLO chromophores, *J. Mat. Chem. C*, 2013, 1, 1144-1159.
7. Cornaton, Y.; Franck, O.; Teale, A. M.; Fromager, E. Analysis of double hybrid density functionals along the adiabatic connection. *Mol. Phys.* 2013, 111, 1275-1294.
8. Hohenberg, P.; Kohn, W. Inhomogeneous electron gas. *Phys. Rev.* 1965, 136, B864-B871.
9. Kohn, W., Sham, L. J. Self-consistent equations including exchange and correlation effects, *Phys. Rev.* 1965, 140, A1133-A1188.
10. Jones, R. O.; Gunnarsson, O. The density functional formalism, its application and prospects. *Rev. Mod. Phys.* 1989, 61, 689-746.
11. Lakshmi Praveen, P., Ojha, D. P. Structure and electronic absorption spectra of nematogenic alkoxy-cinnamic acids – a comparative study based on semiempirical and DFT methods. *J. Mol. Model.* 2011, 18, 1513-1521.
12. Lakshmi Praveen, P., Ojha, D. P. Structure and electronic absorption spectra of nematogenic alkoxy-cinnamic acids – a comparative study based on semiempirical and DFT methods. *Mat. Chem. Phys.* 2012, 135, 628-634.
13. Neese, F. A. A spectroscopy oriented configuration interaction procedure. *J. Chem. Phys.* 2003, 119, 9428-9444.
14. Franke, R. *Theoretical Drug Design Methods*; Elsevier: Amsterdam, 1984; pp 115-123.